A NOVEL SINGLE STAGE THREE PORT CONVERTER AND THREE DOMAIN DISTRIBUTION CONTROL METHOD FOR PV-BATTERY POWERED BACKUP SYSTEM

S. Rajeshwari[1] and Rani Thottungal[2]

[1]Associate Professor, Department of Electrical and Electronics Engineering, INFO Institute of Engineering,
[2]Head of the Department, Department of Electrical and Electronics Engineering Kumaraguru College of Technology
Coimbatore, Tamil Nadu, India
[1] rajimsvicky1996@gmail.com

Abstract

This research work is intended to propose a novel single stage three port converter named boost bidirectional buck with buck boost converter(B4C) for interfacing the Photovoltaic(PV) port, battery port, and load port simultaneously in a power system. The major advantage of the proposed converter topology is the single-stage power conversion which improves the overall effectiveness of the converter. In order to minimize the current conduction losses, the proposed converter is designed with minimal number of power devices. Finally, the performance of the proposed system is simulated in MATLAB and the simulation results are verified by implementing a prototype hardware model. In both cases the converter output voltage is maintained constant when the battery is charging and discharging condition. Moreover, to prove the dynamic performance of the proposed converter based on the overall component count, losses and efficiency a control method based on three domain distribution is also proposed. The simulation results proved that the proposed converter works satisfactorily in all the three-domain distribution methods wherein the load voltage is regulated in all power flow situations.

Keywords: Three port converter, Photovoltaic (PV) Power System, Battery Power Management, Single Stage Power Conditioning System, three domain distribution Control method

I. Introduction

The drastic increase in global energy demand and the rapid depletion of traditional fossil fuel resources, has resulted in solar energy becoming one among the most popular renewable energies [1]. But, because of the changing environmental condition like temperature and solar irradiation, the P–V characteristics curve shows inconsistent Maximum Power Point (MPP), thus imposing a challenge to the tracking issue. In addition, the situation becomes more complex when the array is treated to partial shading, i.e., a condition where a portion or the entire module of the PV array gets non uniform insolation [2]. The sudden variation of solar insolation has led to the reduction in the rated solar power and the respective P–V curves are illustrated in Fig.1. As a consequence of this recent trend, the focus is on the backup powered system in order to meet the load requirement. The converter requires to make sure that the demanded power stays within the limit of the maximum availability to avoid any failure, shut down, or damage [6]–[10] and an efficient converter is necessary for satisfying this operation.

During the partial shading condition, few techniques supporting the backup source were studied in [3]-[5]. This paper evaluates a super capacitor or battery as energy storage device and a bidirectional dc/dc converter were employed to meet up with the power demand. Among the different arrangements of photovoltaic technology, a stand-alone photovoltaic (PV)-battery-powered backup system can be used in different kinds of applications [6], [7].

A rechargeable battery is generally brought into use in the system for saving energy when the solar energy that is produced exceeds the energy which is required by the load. The stored energy can be useful for maintaining the system operation during the shading to the PV panel.

The fundamental two stage single-phase power conditioning system has been considered in general and been analyzed in several technical papers [8]-[11] as indicated in Fig. 2. Nonetheless, the basic two stage single-phase power conditioning system faces setbacks like as being heavy, uneconomic, and inefficient owing to its cascaded power conversion stages (i.e., Unidirectional and Bidirectional).
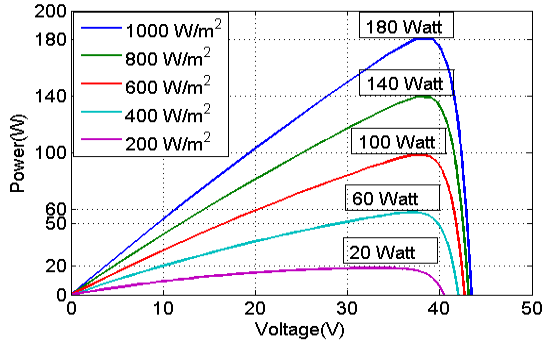
Fig. 1 P-V curve

Modular structured single stage bi-directional converter concepts are in trend for the purpose of reducing costs and providing high reliability. This trend impacts dc–dc battery tied bidirectional converter topologies in a significant manner in terms of minimizing the size and number of semiconductor devices like metal–oxide–semiconductor field-effect transistor (MOSFET), insulated–gate–bipolar–transistor (IGBT) etc., as in fig 2b. Currently, three-port converters, interfacing one PV port, one bidirectional battery port, and one load port of a PV-battery dc power system, are good options for such renewable power system, specifically for spacecraft power supply system. Due to the high power density and the benefit of high efficiency of the three-port converters, it has drawn considerable research interest towards various kinds of applications [12]–[15].
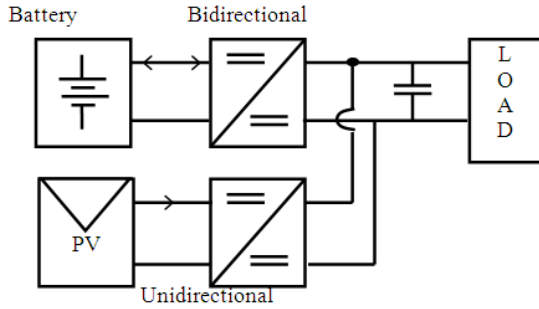

Fig. 2 Power conditioning system architecture

The topology presented in [16] and [17] comprises of two bidirectional boost converters, where the outputs are connected in parallel and also share the output capacitor. This topology characterizes higher efficiency, though the voltage of the PV and battery port must be lower rather than that of the load port, and causing the output current controlling and current sharing to be tedious. In [18], a three switch bidirectional topology was proposed. The current of all the three ports is contiguous, and the switch number is optimized, thereby gaining a more compact design. In [19]–[21], the simple and cost efficient approach that is based on a buck or a buck–boost topology was introduced. But, these converters do not have power flow path for charging on connecting a

battery, and hence not suitable for a PV-battery dc power system.

The converter presented in [22] can interface between two unidirectional input power ports and a bidirectional port for a storage element. Only two power inductors have been used; however, the number of MOSFET and power diode goes up to eight. In [23], a three port converter with high-voltage gain has been presented, and the port current of the converter on the low-voltage side can be continuous. But, semiconductor power devices reaches seven, which will, in turn make the whole system design complicated. In [24] a modified three port type single stage converter (B3C) has been presented as shown in Fig. 3, a fundamental single stage battery that is tied to bidirectional converter has been proposed, consequently the converter works in CCM mode, the components and current conduction devices are also maximized during complete operation, however at an instant of battery charge and discharge the losses incurred; hence attaining high efficiency is complicated here.

In this paper to alleviate above mentioned problems the new topology boost bidirectional buck with buck boost Converter (B4C) is proposed, and its working principles are presented in Section II. The detailed modelling and design formulation is provided in Section III. In Section IV, the B4C control strategies for different domains are explained. Section V provides the Mat Lab simulation verifications and efficiency of proposed B4 converter compared with conventional B3converterto be analyzed.
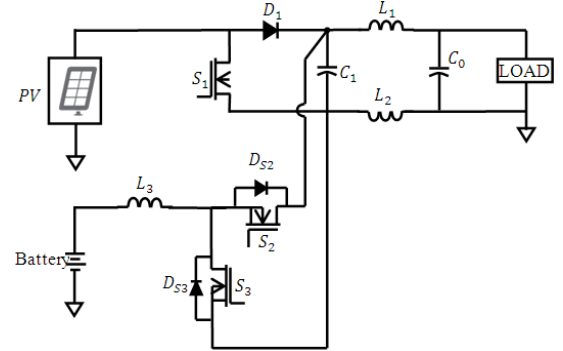

Fig. 3 Conventional B3C architecture [24]

II. Proposed Methodology

The proposed B4C schematic diagram is given in Fig. 4.It chiefly consists of boost converter and bidirectional buck with buck boost converter (B3C). Here, the input inductor (L_1), diode (D_1) and switch (S_1) (boost converter) is utilized for extracting the maximum power from PV panel by making use of maximum power point tracking (MPPT) algorithm.

In addition, B3C arrangement comprising of diode (D_2), buck boost inductor (L_2), switch (S_2), buck inductor (L_3), standalone battery powered backup supply and

output capacitor (C_0)is illustrated in Fig.4.Here, B3C is employed for maintaining the constant output voltage (V_L) arising due to mismatch between the production and demand. When the demand goes beyond than generation, (V_L) drops from its reference value, subsequently battery will discharge in order to provide for the additional demand. Just like that, when the demand is less than generation, (V_L) increases over its reference value, and then consequently the battery will charge in order to absorb the additional power. Buck–boost converter is utilized as a bidirectional converter for the purpose of enabling the bidirectional power flow between load and battery.

The chief achievements of this proposed B4C are as given: 1) Current in the proposed B4C is in discontinuous conduction for improving the life time of the battery. 2) Owing to the single-stage power conversion existing between PV and load ports or between battery and load ports, the effectiveness of the converter gets highly improved. 3) The converter design along with minimal number of components is introduced for reducing the current conduction losses. 4) On the basis of the three-domain load voltage control method, the load voltage is regulated always with high quality in all power flow situations.
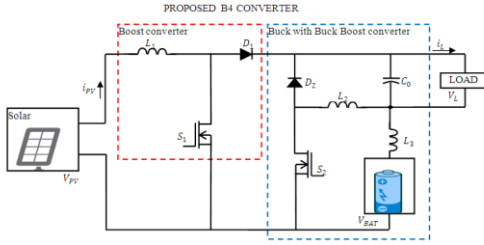

Fig. 4 Proposed B4 converter schematic diagram

Working Principle of Proposed B4C

Based on the relationship that exists between PV generation power and load demand power, B4C will operate in different power flow modes.

The principles of circuit operation and analysis are given assuming the following: 1) All switches are assumed to be in ideal state; 2) the capacitors are sufficiently large such that the voltage ripples because of switching can be neglected and could be considered as constant voltage sources. On the basis of the assumptions above, the converter operation during one switching cycle can be segregated into five unique intervals and the respective equivalent circuits at different operation intervals are illustrated in Fig.5 (a-e).

Mode 0

When switches (S_1) is in "ON" and (S_2) is ''OFF'' condition, the input side inductor L_1 begins charging, and current i_{L1} increases, when simultaneously the inductor L_2 commences discharging via diode D_2 in order to charge

the output capacitorC_0.Hence, the current in inductor L_2 decreases, whereas the output voltage V_L increasesas shown in Fig. 5a.
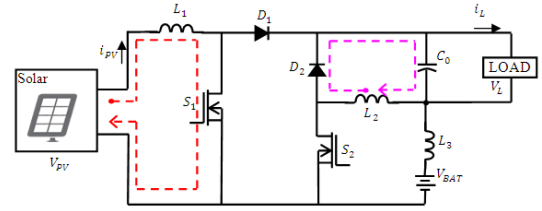

Fig. 5a. Mode 0 operation stage of proposed B4C

Mode 1
This mode is the DCM of operation since the current in inductor L_2 becomes zero, as illustrated in Fig. 5(b). Once switches (S_1) is in "ON" and (S_2) is ''OFF'' condition, the input side inductor L_1 starts to charge, and current i_{L1}increases.
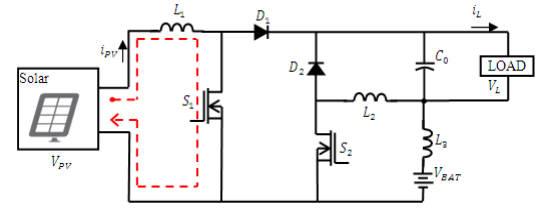

Fig. 5b. Mode 1 operation stage of proposed B4C

Mode 2
When switches S_1 is in "OFF" and S_2 is ''OFF'' condition, the current in PV array i_{PV} and current in input inductor i_{L1} discharges to the output capacitor C_0 and battery through diode D_1, as illustrated in Fig. 5(c),when at the same time the output voltage V_L continues to make an increase in this mode of operation.
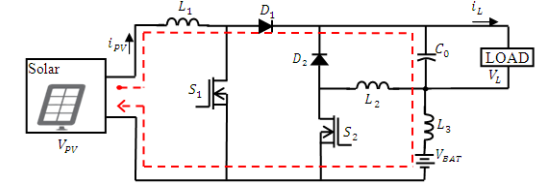

Fig. 5c. Mode 2 operation stage of proposed B4C

Mode 3
When switches (S_1) is in "OFF" and (S_2) is ''ON'' condition, the output capacitor C_0begins Charging from current in PV array and inductor L_1through diode D_1 and switch S_2, when simultaneously the inductor L_2 begins charging via the switch S_2 and inductor L_3, and current i_{L2} increases as shown in Fig. 5d.
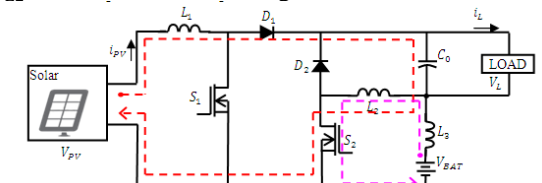

Fig. 5d. Mode 3 operation stage of proposed B4C

Mode 4

When switches (S_1) is in "ON" and (S_2) is ''OFF'' condition, as per the higher potential of diode D_2, diode D_1 is reverse biased. Whereas the inductor L_2 begins discharging via diode D_2, in order to charge the output capacitor C_0, and the output voltage V_L increasesas shown in Fig. 5e.
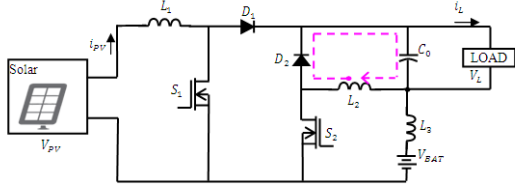

Fig. 5e. Mode 4 operation stage of proposed B4C

Fig. 5 Operation stages of proposed B4C

Design Procedure of B4C

Design of inductors and output capacitor

Assuming that an ideal lossless converter operates in the steady state and operates in the discontinuous conduction mode (DCM), the design procedure of proposed B4C is analysed based on following mathematical equation.

Design of input inductor or boost inductor (L_1)

$$L_1 = \frac{V_{in}*D}{f_{sw}*\Delta i_{L1}} \tag{1}$$

Where, D is the duty cycle i.e. $D = \frac{V_L - V_{in}}{V_L}$, V_{in} denotes input voltage from panel, f_{sw} denotes switching frequency of the carrier signal, similarly Δi_{L1} represents ripple current of inductor L_1.

$$\Delta i_{L1} = \frac{V_{in} - (V_{L_1} + (i_{L_1}*R_L))}{L_1} * T_t \tag{2}$$

Where, V_{L_1}, i_{L_1}, R_L and T_t denotes voltage and current across the inductor L_1, load resistor and total time respectively.

Here $i_{L_1} = \frac{V_L}{R_L}$

Assume average voltage of inductor $V_{L_1} = 0$, Where V_L denotes Load Voltage.

Design of buck boost Inductor (L_2)

$$L_{2(BUCK)} = \frac{V_L*(V_{in(max)} - V_L)}{K_{L_2}*f_{sw}*V_{in(max)}*i_L} \tag{3}$$

Where $V_{in(max)}$ represents maximum input voltage generated from PV panel at standard test 1000 w/m^2 Irradiation Condition (STC). i_L Represents output current (rated Load Current), K_{L_2} denotes estimated co-efficient i.e. amount of inductor L_2 ripple current relative to the maximum output current ($0.2 < K_{L_2} < 0.4$).

Similarly,

$$L_{2(Boost)} = \frac{V_{in(min)^2} (V_L - V_{in(min)})}{f_{sw}*K_{L_2}*i_L*V_L^2} \tag{4}$$

Where $V_{in(min)}$ denotes minimum input voltage, i.e. input voltage generated from PV panel at low irradiation

condition. Similarly, inductor L_3 design is equivalent to the buck boost inductorL_2.

Design of output capacitor (C_0)

$$C_0 = \frac{i_L*D}{f_{sw}*\Delta V_L} \tag{5}$$

Where ΔV_L represents desired output voltage ripple.

Switching current calculation of S_1 and S_2

The power device can be selected by considering some acceptable voltage and current margins. The current value of switching devices is calculated by following equations.

$$i_{S_1} = \frac{\Delta i_{max}}{2} + \frac{i_L}{1 - D_{max}} \tag{6}$$

Where Δi_{max} and D_{max} denotes maximum ripple current and maximum duty cycle respectively.

$$\Delta i_{max} = \frac{V_{in(min)}*D_{max}}{f_{sw}*L_1} \tag{7}$$

Similarly,

$$i_{S_2} = \frac{\Delta i_{max}}{2} + i_L \tag{8}$$

$$\text{Here } \Delta i_{max} = \frac{V_{in(max)}*D_{min}}{f_{sw}*L_3} \tag{9}$$

Where D_{min} represents minimum duty cycle.

Based on the equations above, values of all the inductors can be selected according to the current ripple specification, and the values of all the capacitors can be selected according to the voltage ripple specification.

Proposed B4C Control Strategy

Usually, the load port of the converter must be regulated tightly to satisfy the load requirements, the PV port has to deploy maximum power tracking in order to harness the maximum energy when the load power is bulky, and the battery port charging current should be controlled in order to implement the battery management.

Two control degrees of freedom are required to implement those tasks. One of them regulates the load port current for load port voltage regulation or controls the PV port voltage, thus making PV operate in MPPT mode. The other freedom has the control over the current of L1 in order to regulate the charging and discharging power with the goal of battery management realization when sunlight or load port voltage varying conditions. In this paper, the first control degrees of freedom is having the control over the load port current or the PV port voltage by PWM-S_1, and the other freedom is controlling the bidirectional current of L3 by PWM-S_2.

Fig. 6 illustrates the control diagram and modulation technique for the proposed converter, where V_{PV}^* refers to the output of the MPPT algorithm (employing the perturb and observe method), V_{PV} denotes the voltage of PV, IVRC represents the PV input voltage regulation controller, for output voltage regulation, the output voltage is measured and the comparison is made with a voltage reference (whose voltage will always be a

constant). The voltage difference, or regulation error, is amplified in accordance to the proportional and integral gains of the output voltage regulation controller (OVRC), delivering a control voltage referred to as V_C. V_C denotes the output of OVRC, i_L represents the output current of the converter's load port, OCRC denotes the bus port of output current regulation controller.

IBAT_REF and VBAT_REF are the output of the battery management unit (BMU) whose function is the control of the battery's constant current or constant voltage, IBAT denotes the battery charging or discharging current (bidirectional current measuring used here), and BVR and BCR are the corresponding battery voltage regulation and battery current regulation.
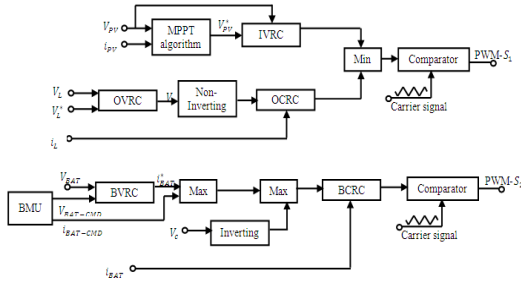

Fig. 6 Control strategy of B4C

III. Results and Discussions

The performance of the proposed B4C is modelled in a matlab / Simulink environment making use of the Sim Power-System Toolbox. The proposed converter performance is analysed under dynamic solar irradiation conditions. Parameters like Panel power(P_{PV}), Load power(P_L), Battery power(P_{BAT}), Load voltage(V_L), then (i_{L1}), (i_{L2}) and (i_{L3}) current flowing through the inductors L_1, L_2 and L_3 respectively, and then finally state of charge in the battery (SOC) of the proposed converter are assessed in order to show its proper functioning. The converter input and output specifications employed for the simulations are provided in Table 1. Furthermore, dynamic irradiation based domain distribution is illustrated in fig 7.
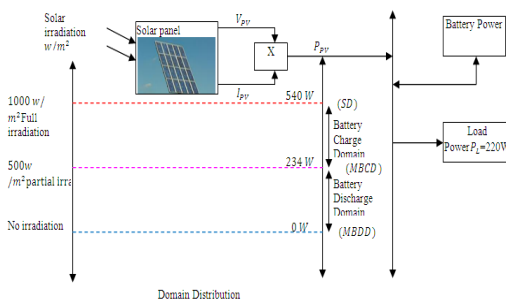

Fig. 7 Domain Distribution Architecture

As per the domain distribution as illustrated in Fig. 7, solar irradiation 1000w/m2 refers to the proposed converter functions in Sun Domain (SD), when the solar irradiation suddenly is reduced from 1000w/m2 to 500w/m2 owing to environmental conditions. The proposed converter operates in Minimum Battery Charge Domain (MBCD), subsequently during night time (no irradiation from the sun) the proposed converter operates in Maximum Battery Discharge Domain (MBDD).The converter in these three domains performs on the basis of solar irradiation; therefore, the load voltage can be regulated, and the modes can be adjusted automatically as per the power conditions of each port. These three respective domains results are examined below in detail.

Table 1 B4C topology simulation specifications

Parameter	value
180W PV panel design specification	
Short circuit current at reference condition Isc	5.48 A
Open circuit voltage at reference condition Voc	43.6 V
MPP voltage at reference condition Vmp	35.8 V
MPP current at reference condition Imp	5.03 A
Series resistance Rs	0.1133
Irradiance at standard test conditions (STC)	1000 W/m2
Cell temperature at standard test conditions	25 _C
Maximum power @ STC	180W
Input output specification	540W
Input power (three 180W panel connected in series configuration)	220W
Load power	200V
Load voltage	

3.1 Sun Domain

The solar generation power is enough to supply for the load and for charging the battery, as indicated in

$$P_{PV} \geq i_{BAT-CMD} * V_{BAT} + P_L \tag{10}$$

Where V_{BAT}, i_{BAT} and $i_{BAT-CMD}$ denotes the battery voltage, battery current and command of battery current respectively.

Figure 8 and 9 clearly depicts the proposed converter functions in SD. Assume the maximum irradiation (1000w/m2) is received, the respective panel power (540 W) is illustrated in fig 8(a).The load power and load voltage is kept at 220 W and 220 V respectively as indicated in figure 8(b) and 8(d). The additional power of panel (300 W) is stored efficiently in the storage battery as per the command of battery management unit as shown in figure 8(c). As seen from the figure 8(c) the negative sign is an indication that the, storage battery receives the energy from the panel. In addition, the current flowing through the inductors (L_1-L_3) and state of charge in the battery for verifying the proposed

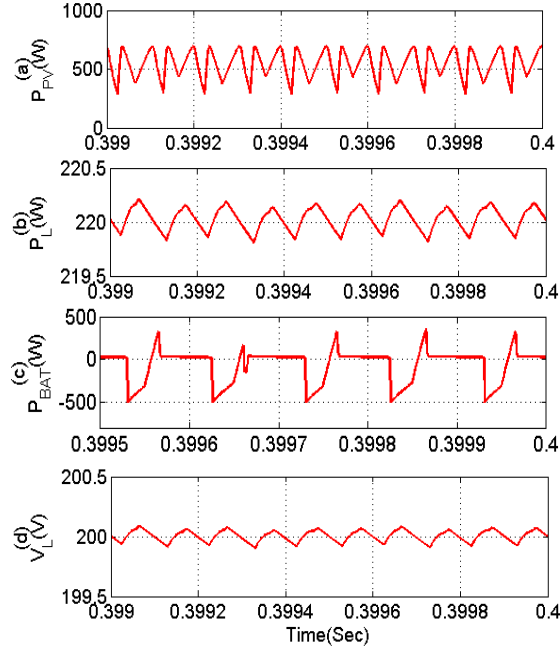converter to operate in SD is shown in figure 9(a)-9(d) respectively.

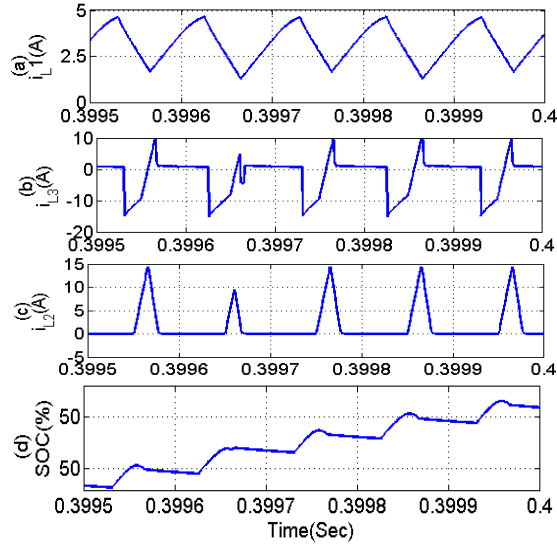Fig. 8 Power and voltage waveforms of B4C operates in SD

Fig. 9 Inductor current and SOC waveforms of B4C operates in SD

3.2 Minimum Battery Charge Domain

The solar generation power is sufficient to supply the load and not adequate to charge the battery, as is indicated in

$$P_L \cong P_L \qquad (11)$$

Where (P_{PV}) and (P_L) denotes the Panel power and load power respectively.

Fig. 10 and 11 clearly depicts the proposed converter functions in MBCD. Here the medium irradiation (500w/m2) is focused; the respective panel power (234W) is illustrated in Fig 10(a). The load power and load voltage is maintained at 220 W and 220 V respectively as indicated in Fig 10(b) and 10(d). Owing to medium irradiation of solar panel the proposed converter is not capable of charging the battery sufficiently, and the respective battery power is indicated in figure 10(c).Furthermore, the current flowing through the inductors (L_1-L_3) and state of charge in the battery in order to verify the proposed converter operating in MBCD is shown in Fig. 11(a)-11(d) respectively.
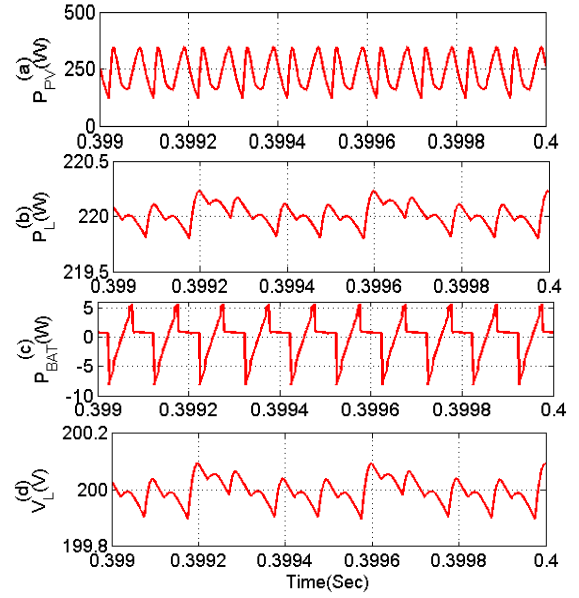

Fig. 10 Power and voltage waveforms of B4C operates in MBCD
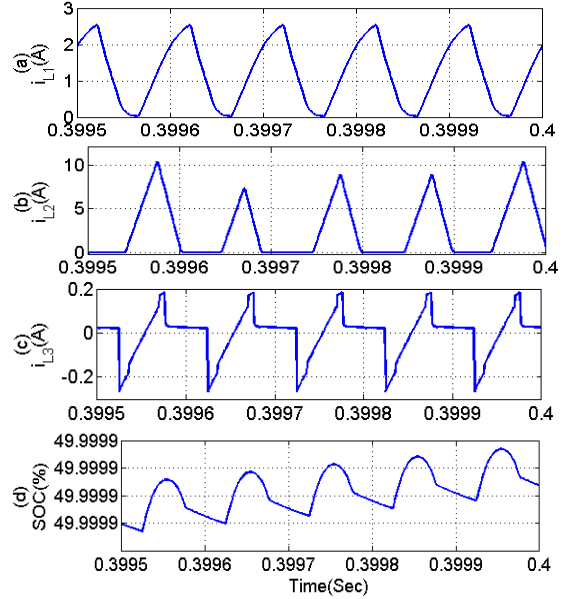

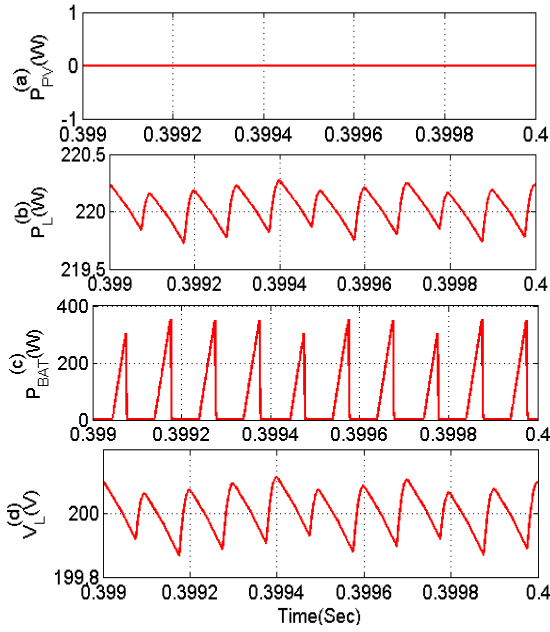Fig 11 Inductor current and SOC waveforms of B4C operates in MBCD

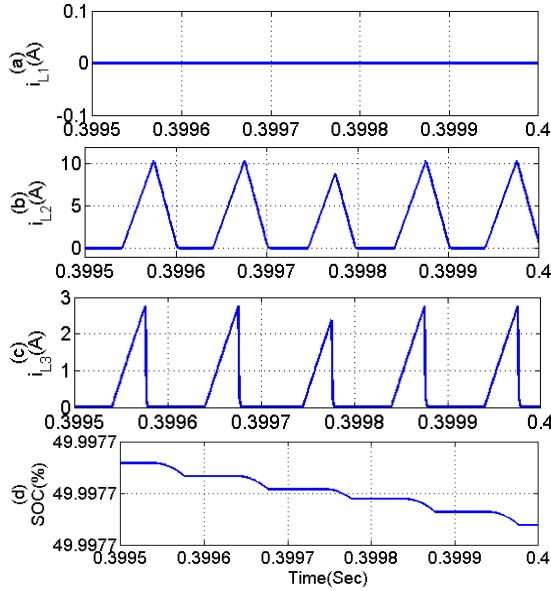Fig. 12 Power and voltage waveforms of B4C operates in MBDD

Fig. 13 Inductor current and SOC% waveforms of B4C operates in MBDD

3.3 Maximum Battery Discharge Domain

There is absence of power from solar (during night time); hence battery should supply the load power demand, as shown in

$$P_{PV} \leq P_L \qquad (12)$$

The proposed converter operates in the MBDD as illustrated in Fig 12 and 13. The load port voltage will be regulated by adjusting the discharging current

accordingly. The discharging current will be controlled in order to meet

$$P_{PV} + I_{dis} * V_{BAT} = P_L \qquad (13)$$

Where I_{dis} is the discharging current of the battery.

Here no irradiation from the solar panel is taken into consideration as shown in Fig 12(a). The load power and load voltage is maintained at 220 W and 220 V respectively as indicated in figure 12(b) and 12(d). Owing to the unavailability of power from solar panel the proposed converter works in MBDD. The battery powered backup supply must be able to support the load port power enough, and the respective battery power is illustrated in Fig. 12(c).In addition the current flowing through the inductors (L_1–L_3) and state of charge in the battery for verifying the proposed converter operating in MBDD is shown in figure 13(a)-13(d) respectively. Based on the analysis above, the operation mode can be decided as per the current energy conditions like available solar power, load demand power, and battery management command.

Comparative Analysis of Proposed B4 Converter with Conventional B3 Converter

A brief components comparison of the proposed B4Cconfiguration with the B3C configurations is tabulated in Table 2. It shows the total number of devices (Switch—S, Diode—D, Inductor—L, and Capacitor—C). As seen from the Table 2 The proposed B4C has comparatively lower number of components and least number of conducting devices when the B4C is operating in different distribution domains, resulting in the overall converter size minimization and improving the suitability of the proposed B4C.

Table 2 component comparison of B3 and B4 converter

Configuration	No of Devices				
	S	D	L	C	Total
CONVENTIONAL B3 CONVERTER [25]	3	3*	3	2	11
PROPOSED B4 CONVERTER	2	2	3	1	8
*denotes including anti parallel diode of MOSFET					

Similarly a brief (Losses, Component Conduction and Efficiency) comparison of the proposed B4C with the traditional B3C when working in different distribution domain (Fig. 7) is tabulated in Table 3

Table 3 Comparison of component conduction of B3 and B4 converter when operating in different distribution domain

Particulars	Conventional B3 Converter [24]	Proposed B4 converter
Current conduction Devices when converter operates in SD	9	5
Current conduction Devices when converter operates in MBCD	6	8
Current conduction Devices when converter operates in MBDD	7	4
Overall Component conduction counts when converter operates in all distribution domains	22	17
Losses when converter operates in SD	32.4W	19.98W
Losses when converter operates in MBCD	9.8W	12.87W
Losses when converter operates in MBDD	11.54W	10.84W
Average Losses when converter operates in all distribution domains	53.74W	43.69W
Average Efficiency when converter operates in all distribution domains	94.2%	96.3%

It is evident from the table, that the proposed B4C performance is superior in comparison with the conventional B3C when operating in all different distribution conditions.
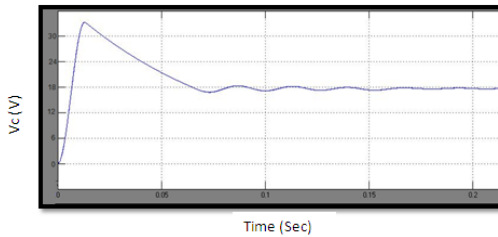

Fig 14 . Voltage during boosting operation

The simulation output of the converter voltage (Vc) during boosting operation is shown in Fig.14. From the output it is evident that, Vc increases and settles at 18 V , which confirms the boosting operation of the system. The same is compared with the measured hardware results and found to be satisfactory.

IV. Hardware Implementation

Hardware Implementation is done by constructing a prototype model (Fig.15) with normal power supply unit, a driver circuit which consists of a transistor BC 547 is capable of handling 500 mA. Optocoupler is used to emit the input. This input is regulated by the voltage regulator IC 7805 and this regulated output is given to MOSFET for switching operation. The output from the driver

circuit is fed to the control unit consists of a controller DSPIC 3074011 it is a 40 PIN IC. Capable of handling 5 V supply. A 20 mHz oscillator is used to reduce the execution time .The successful verification of the hardware model output against simulation, proves the results such that when the battery is charging , boosting operation is performed and the converter output voltage level is increased to 18 V. When the battery i s discharging with a help of buck with buck boost converter, the output   voltage level is also maintained constant at 18 V.
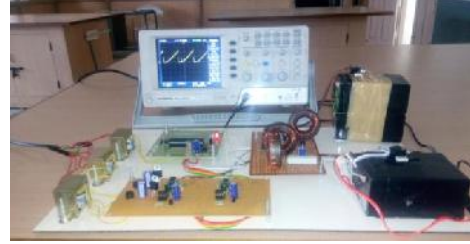

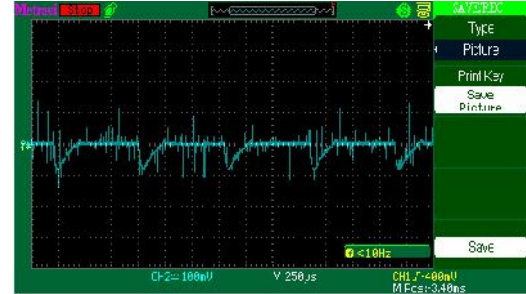Fig 15 . Hardware Implementation of B4C
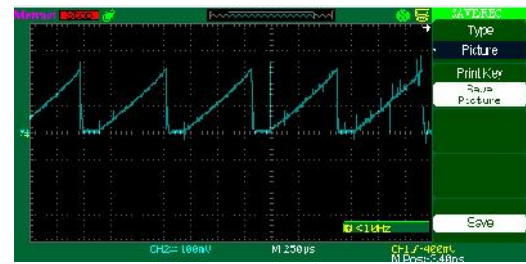

Fig 16. Battery Charging

Fig 17. Battery Discharging

V. Conclusion

In this paper, a boost bidirectional buck with buck boost Converter (B4C) and its operation stages, consequently control method have been proposed by interfacing a PV port, a battery port, and a load port (three port) simultaneously. The working principle and design procedure of the proposed B4C has been analysed in detail. Furthermore the three domain distribution control based simulation results has been given for evaluate the dynamic performance of proposed B4C. Finally, effectiveness (overall component count, losses and efficiency) of the proposed B4C topology has been observed to outperform the conventional B3C topology. The proposed topology can be applied in several applications such as electric vehicles, street light, micro inverter system, and so on.

References

[1] Vaona, A. The effect of renewable energy generation on import demand. Renewable energy, 2016; 86: 354-359.

[2] Ishaque, K; salam, Z. A deterministic particle swarm optimization maximum power point tracker for photovoltaic system under partial shading condition, ieee transactions on industrial electronics, 2013; 60(8): 3195-3206.

[3] Lai, J.S. Power conditioning circuit topologies, ieee ind. Electron.mag., 2009; 3(2): 24-34.

[4] Horizon fuel cell technologies, h-series pemfc system user guide, 2010; available in http://www.horizonfuelcell.com.

[5] Cano, A; jurado, F; sánchez, H; fernández, L.M; castañeda, M. Optimal sizing of stand-alone hybrid systems based on pv/wt/fc by using several methodologies original research article journal of the energy institute, 2014; 87(4):330-340.

[6] Caracas, J. M; farias, G. D. C; Teixeira, l. M; ribeiro, l. D. S. Implementation of a high-efficiency, high-lifetime,and low-cost converter for an autonomous photovoltaic water pumping system, IEEE trans. Ind. Appl., 2014; 50 (1):631-641.

[7] Elgendy, M; zahawi, B; atkinson, D. Assessment of perturb and observe mppt algorithm implementation techniques for pv pumping applications, ieee trans. Sustain. Energy, 2012; 3(1): 21-33.

[8] Lee, J; Jo, J; choi, S; han, S.-B. A 10-kw SOFC low-voltage battery hybrid power conditioning system for residential use, ieee trans. Energy convers., 2006; 21(2):575-585.

[9] Thounthong, p; davat, b; rael, s; sethakul, p. Fuel cell high-power applications, ieee ind. Electron. Mag., 2009; 3(1):32-46.

[10] Alcazar, Y. J. A; bascopé, R. T; de oliveira, D. S; Andrade, E. H; cárdenas, W.G. High voltage gain boost converter based on three-state switching cell and voltage multipliers. In industrial electronics, iecon. 34th annual conference of ieee. 2008; 2346-2352.

[11] Pérez-navarro, D. Alfonso, H.E. Ariza, J. Cárcel, A. Correcher, G. Escrivá-escrivá, E. Hurtado, F. Ibáñez, E. Peñalvo, R. Roig, C. Roldán, C. Sánchez, I. Segura, C. Vargas experimental verification of hybrid renewable systems as feasible energy sources original research article renewable energy, volume 86, february 2016, pages 384-

[12] Jiang, W; fahimi, B. Multiport power electronic interface—concept, modeling, and design, ieee trans. Power electron., 2011; 26(7): 1890-1900.

[13] Y. M. Chen, A. Q. Huang, and x. Yu, a high step-up three-port dc-dc converter for stand-alone pv/battery power systems, ieee trans. Power electron., vol. 28, no. 11, pp. 5049-5062, nov. 2013.

[14] Wang, z; li, h. An integrated three-port bidirectional dc-dc converter for pv application on a dc distribution system, ieee trans. Power electron., 2013; 28: 4612-4624.

[15] Wu, h; sun, k; chen, r; hu, h; xing, y. Full-bridge three-port converters with wide input voltage range for renewable power systems, ieee trans. Power electron., 2012; 27(9): 3965-3974.

[16] Di napoli, a; crescimbini, f; solero, l; caricchi, f; capponi, f. G. Multiple-input dc-dc power converter for power-flow management in hybrid vehicles, in conf. Rec. Ieee ias annu. Meeting, 2002; 1578- 1585.

[17] Di napoli, a; crescimbini, f; rodo, s; solero, l. Multiple input dc-dc power converter for fuel-cell powered hybrid vehicles, in proc. 33rd annu .ieee power electron. Spec. Conf., 2002; 1685-1690.

[18] Marchesoni, m; vacca, c.new dc-dc converter for energy storage system interfacing in fuel cell hybrid electric vehicles, ieee trans. Power electron, 2007; 22(1), 301-308.

[19] Rodriguez f. D; imes, w. G. Analysis and modeling of a two input dc/dc converter with two controlled variables and four switched networks, in proc. 31st intersoc. Energy conv. Eng. Conf., 1996; 322-327.

[20] Dobbs b. G; chapman, p. L. A multiple-input dc-dc converter topology, ieee trans. Power electron., 2003; 1(1): 6-9.

[21] Onwuchekwa c. N; kwasinski, a. A modified-time-sharing switching technique for multiple-input dc-dc converters, ieee trans. Power electron., 2012; 27(11): 4492-4502.

[22] Nejabatkhah, f; danyali, s; hosseini, s. H; sabahi, m; niapour, s. M. Modeling and control of a new three-input dc-dc boost converter for hybrid pv/fc/battery power system, ieee trans. Power electron., 2012; 27(5):2309-2324.

[23] Chien, l. J; chen, c. C; chen, j. F; hsieh, y. P. Novel three-port converter with high-voltage gain, ieee trans. Power electron., 2014; 29(9):4693-4703.

[24] Zhu, h; zhang, d; zhang, b; zhou, z. A nonisolated three-port dc-dc converter and three-domain control method for pv-battery power systems. Ieee transactions on industrial electronics, 2015; 62(8):4937-4947.